Inorganic Chemistry

pubs.acs.org/IC

Article

Rhenium-Imido Corroles

Abraham B. Alemayehu, Simon J. Teat, Sergey M. Borisov, and Abhik Ghosh*

Cite This: *Inorg. Chem.* 2020, 59, 6382−6389

Read Online

ACCESS | Metrics & More | Article Recommendations | Supporting Information

ABSTRACT: Metallocorroles involving 5d transition metals are currently of interest as near-IR phosphors and as photosensitizers for oxygen sensing and photodynamic therapy. Their syntheses, however, are often bedeviled by capricious and low-yielding protocols. Against this backdrop, we describe rhenium-imido corroles, a new class of 5d metallocorroles, synthesized simply and in respectable (∼30%) yields via the interaction of a free-base corrole, $Re_2(CO)_{10}$, K_2CO_3, and aniline in 1,2,4-trichlorobenzene at ∼190 °C in a sealed vial under strict anaerobic conditions. The generality of the method was shown by the synthesis of six derivatives, including those derived from *meso*-tris(pentafluorophenyl)corrole, H_3[TPFPC], and five different *meso*-tris(*p*-X-phenyl)corroles, H_3[T*p*XPC], where X = CF_3, F, H, CH_3, OCH_3. Single-crystal X-ray structures obtained for two of the complexes, Re[T*p*FPC](NPh) and Re[T*p*CF_3PC](NPh), revealed relatively unstrained equatorial Re−N distances of ∼2.00 Å, a ∼0.7-Å displacement of the Re from the mean plane of the corrole nitrogens, and an Re−N_{imido} distance of ∼1.72 Å. Details of the corrole skeletal bond distances, diamagnetic ^{1}H NMR spectra, relatively substituent-independent Soret maxima, and electrochemical HOMO−LUMO gaps of ∼2.2 V all indicated an innocent corrole macrocycle. Surprisingly, unlike several other classes of 5d metallocorroles, the Re-imido complexes proved nonemissive in solution at room temperature and also failed to sensitize singlet oxygen formation, indicating rapid radiationless deactivation of the triplet state, presumably via the rapidly rotating axial phenyl group. By analogy with other metal-oxo and -imido corroles, we remain hopeful that the Re-imido group will prove amenable to further elaboration and thereby contribute to the development of a somewhat challenging area of coordination chemistry.

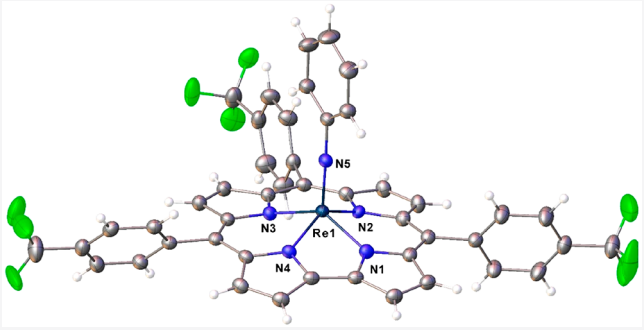

INTRODUCTION

The 5d metallocorroles are an unusual class of complexes that encapsulate a large 5d transition metal ion within a sterically constrained macrocyclic ligand.[1,2] Unsurprisingly in view of the structural mismatch inherent in their structures, their syntheses require highly specific conditions of reagent, solvent, and temperature and typically afford products in poor yields. Even the best conditions for gold insertion are capricious, unusually sensitive to impurities, and afford yields of only about 20%,[3−6] while the yields for platinum insertion are considerably worse,[7,8] well under 5%. These shortcomings notwithstanding, the 5d metallocorroles are of considerable interest. Once synthesized, they are surprisingly rugged. In addition, a number of them exhibit room-temperature near-IR phosphorescence,[9−14] which has led to applications as oxygen sensors[10−12] and as photosensitizers in photodynamic therapy[13,15] and dye-sensitized solar cells.[13] Particularly promising in this regard are the rhenium(V)-oxo corroles, which are accessible both simply and in fairly high yields.[16] Presented herein are a new class of 5d metallocorroles—rhenium-imido corroles—which have now been synthesized in respectable yields. Like Mo^VO,[17] Re^VO,[16] and Ta(V)-imido[18] corroles, the present complexes may also serve as starting materials for new axial ligation chemistry, an aspect of 5d metallocorroles that is still in its infancy.[19,20]

RESULTS AND DISCUSSION

Synthesis and Proof of Composition. Given the extreme oxophilicity of rhenium, the synthesis of rhenium-imido corroles is a potentially tricky proposition. After a fair amount of trial and error, the reaction conditions that we ultimately came up with proved simple. A free-base *meso*-triarylcorrole, $Re_2(CO)_{10}$, K_2CO_3, and aniline, upon heating at ∼190 °C in 1,2,4-trichlorobenzene under strict exclusion of oxygen, afforded the desired rhenium(V)-phenylimido corroles in 28−35% yields along with smaller quantities (<10%) of the corresponding Re^VO corroles (Scheme 1). The generality of the method was shown by the synthesis of six derivatives, including those derived from *meso*-tris(pentafluorophenyl)corrole, H_3[TPFPC], and five different *meso*-tris(*p*-X-phenyl)-

Received: February 14, 2020
Published: April 10, 2020

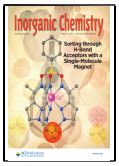

https://dx.doi.org/10.1021/acs.inorgchem.0c00477
Inorg. Chem. 2020, 59, 6382−6389

Scheme 1. Reaction Conditions Leading to Re-phenylimido Corroles

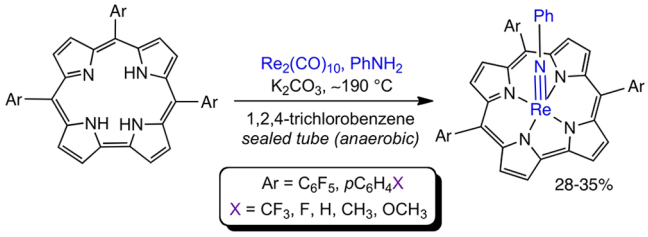

corroles, H_3[T*p*XPC], where X = CF_3, F, H, CH_3, OCH_3. The formation of the desired phenylimido complexes seemed immediately plausible upon mass spectrometric analysis of the crude products, an inference that was soon bolstered by ^{1}H and ^{19}F NMR spectroscopy. Although ^{1}H NMR spectra showed a number of broad signals at room temperature, they sharpened at −20 °C, allowing essentially full assignment of the spectra. This sharpening reflects slowing of *meso*-phenyl rotation at low temperature, resulting in nonequivalent *o*, *o*′ and *m*, *m*′ signals, a phenomenon that has also been observed in $Re^{V}O$,[16] $Os^{VI}N$,[21] and other metallocorroles with a square-pyramidal metal center (Figure 1).

X-ray Crystal Structures. Unambiguous proof of composition and structure of the new complexes came from two single-crystal X-ray analyses (Table 1), which could be obtained for Re[T*p*FPC](NPh) (Figure 2) and Re[T*p*CF_3PC](NPh) (Figure 3). Both structures exhibit domed corrole macrocycles with the Re atom displaced about 0.7 Å (more accurately, 0.693 and 0.694 Å, respectively) above the

Table 1. Selected X-ray Crystallographic Data for the Samples Analyzed

sample	Re[T*p*FPC](NPh)	Re[T*p*CF_3PC](NPh)
chemical formula	C_{43} H_{25} F_3 N_5 Re	C_{55} H_{34} F_9 N_5 Re
formula mass	854.88	1122.07
crystal system	orthorhombic	triclinic
crystal size (mm^3)	0.120 × 0.030 × 0.020	0.200 × 0.150 × 0.040
space group	*Pbca*	$P\bar{1}$
λ (Å)	0.7288	0.7288
a (Å)	8.6866(3)	8.6386(5)
b (Å)	24.1076(8)	16.7410(10)
c (Å)	31.9039(10)	16.7461(10)
α (deg)	90	78.638(2)
β (deg)	90	75.218(2)
γ (deg)	90	77.206(2)
Z	8	2
V ($Å^3$)	6681.1(4)	2258.0(2)
temperature (K)	100(2)	100(2)
density (g/cm^3)	1.700	1.650
measured reflections	203004	87509
unique reflections	8327	11336
parameters	469	660
restraints	0	36
R_{int}	0.0342	0.0405
θ range (deg.)	1.852−29.116	1.969−29.151
R_1, wR_2 all data	0.0287, 0.0756	0.0240, 0.0634
S (GooF) all data	1.041	1.057
max/min res. dens. ($e/Å^3$)	2.582/−1.215	1.377/−1.729

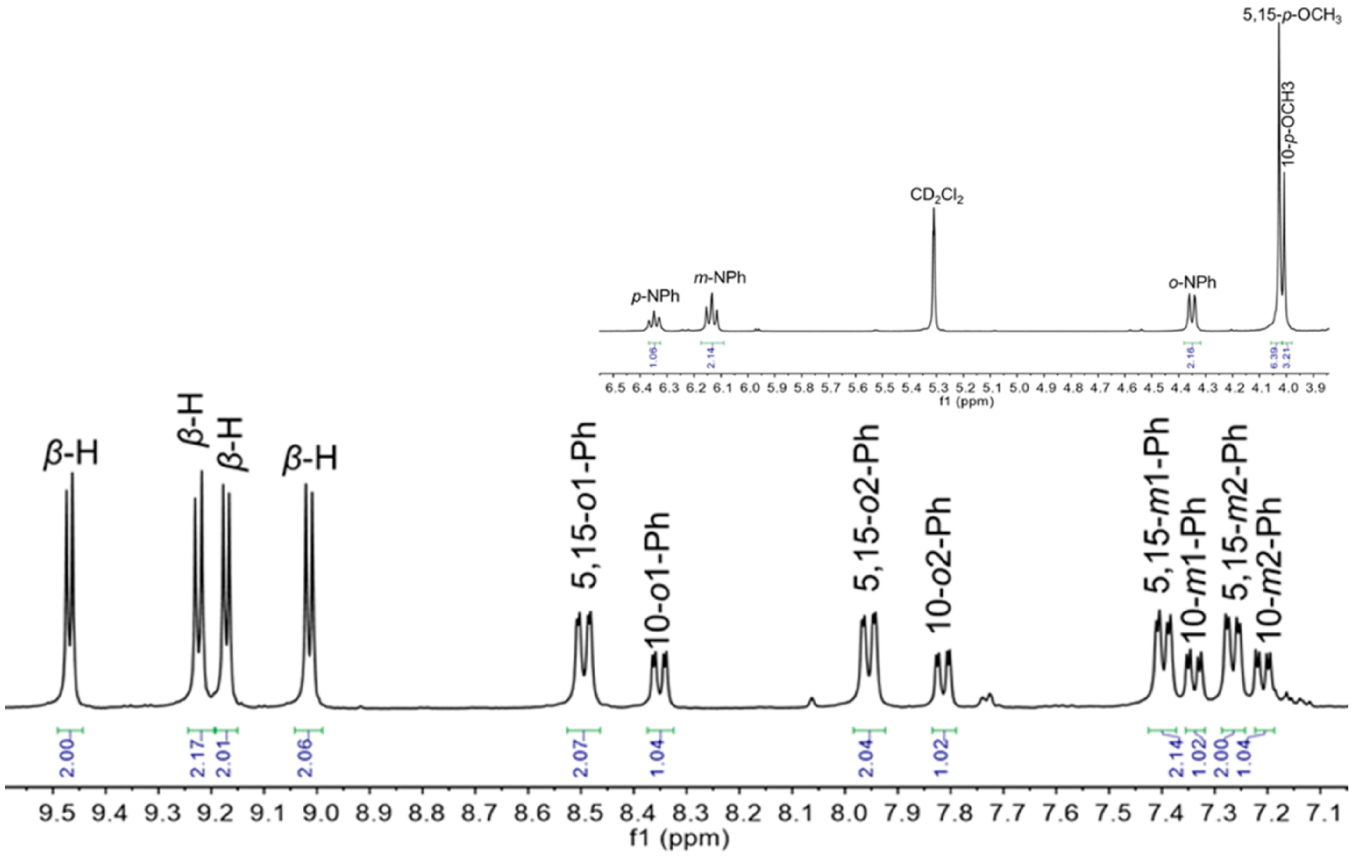

Figure 1. Representative ^{1}H NMR spectrum: Re[T*p*OCH_3PC](NPh).

https://dx.doi.org/10.1021/acs.inorgchem.0c00477
Inorg. Chem. 2020, 59, 6382−6389

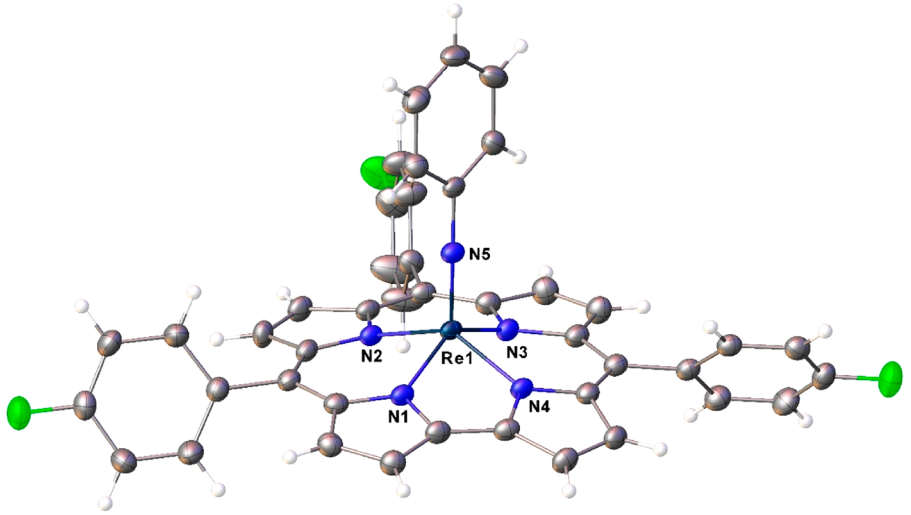

Figure 2. Thermal ellipsoid plot for Re[T*p*FPC](NPh). Selected distances (Å): Re1−N1 1.998(2), Re1−N2 2.017(2), Re1−N3 2.008(2), Re1−N4 2.002(2), and Re1−N5 1.721(2).

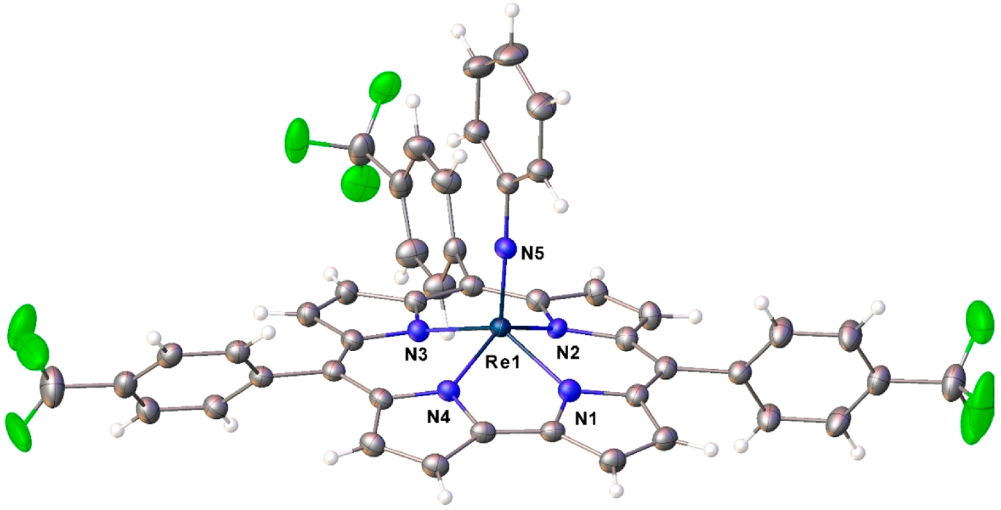

Figure 3. Thermal ellipsoid plot for Re[T*p*CF_3PC](NPh). Selected distances (Å): Re1−N1 2.000(2), Re1−N2 2.009(2), Re1−N3 2.006(2), Re1−N4 2.003(2), and Re1−N5 1.716(2).

mean plane of the corrole nitrogens. The Re−N distances involving the corrole all hover around 2.00 Å, in excellent agreement with the sum of Pyykkö's single-bond covalent radii for Re (1.31 Å) and N (0.71 Å). The Re−N_{imido} distance of ∼1.72 Å is slightly longer than the sum of Pyykkö's triple-bond covalent radii for Re (1.10 Å) and N (0.54 Å), reflecting the fact that the latter radius is largely trained on data for nitrido, as opposed to imido, complexes.[22−24] Overall, the bond distances are suggestive of relatively unstrained Re−N bonds, which may provide a partial explanation for the relative ease of Re insertion into corroles. Finally, the two structures do not exhibit any indication of bond length alternation within and around the bipyrrole part of the molecules, which (if present) would indicate significant noninnocent or corrole$^{\bullet 2-}$ character,[25−29] a phenomenon that is widely observed among metallocorroles.[30]

UV−Vis and Electrochemical Studies. Electronic absorption spectroscopy (Figure 4) and electrochemical studies (Figure 5), summarized in Table 2, provided additional electronic-structural insight. Qualitatively, the electronic absorption spectra of the new complexes resemble those of

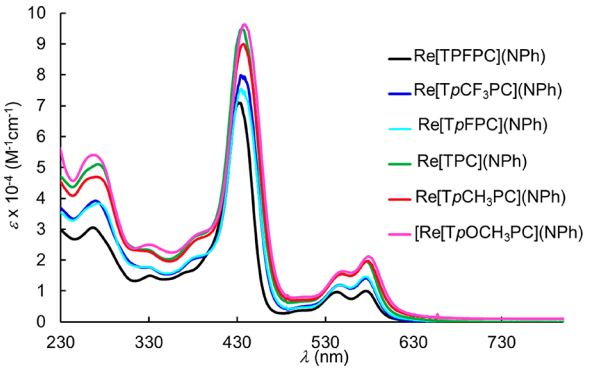

Figure 4. UV−vis spectra of Re-imido corroles in dichloromethane.

their $Re^{V}O$,[16] $Os^{VI}N$,[21] Au^{III},[5] and Pt^{IV} congeners,[8] consisting of sharp Soret bands, distinctive double-humped Q bands, and a couple of weaker features in between. Furthermore, the 434 nm Soret maxima are essentially independent of the *para* substituent on the *meso*-phenyl groups, an observation that has been empirically correlated with an innocent corrole^{3-}

https://dx.doi.org/10.1021/acs.inorgchem.0c00477
Inorg. Chem. 2020, 59, 6382−6389

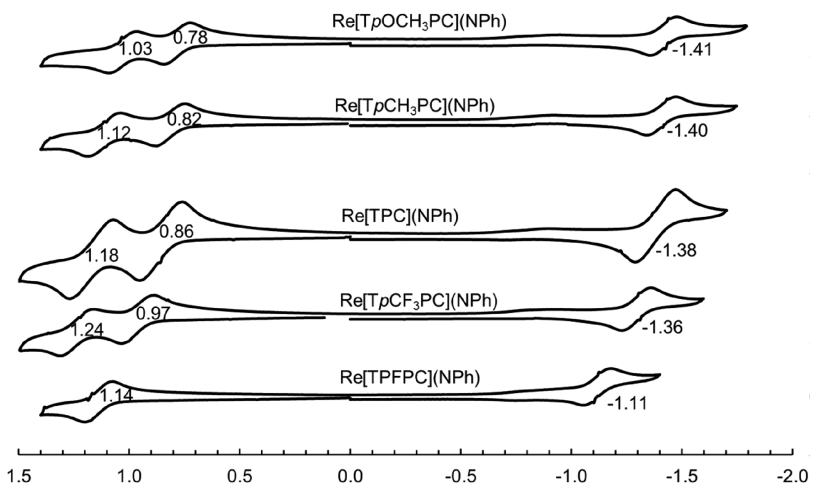

Figure 5. Cyclic voltammograms of Re-imido corroles in CH_2Cl_2 with 0.1 M tetrabutylammonium perchlorate. Scan rate = 100 mV s^{-1}.

Table 2. UV-Vis Absorption Maxima (λ_{max}, nm) and Redox Potentials (V vs. SCE) of Re-imido Corroles

compound	λ_{max}	Q	$E_{1/2\text{-ox2}}$	$E_{1/2\text{-ox1}}$	$E_{1/2\text{-red}}$	ΔE
Re[TPFPC](NPh)	431	544, 577	–	1.14	−1.11	2.25
Re[T*p*CF_3PC](NPh)	434	547, 577	1.24	0.97	−1.29	2.26
Re[T*p*FPC](NPh)	434	548, 575	1.15	0.88	−1.36	2.24
Re[TPC](NPh)	434	458, 576	1.18	0.86	−1.38	2.24
Re[T*p*CH_3PC](NPh)	434	549, 578	1.12	0.82	−1.40	2.22
Re[T*p*OCH_3PC](NPh)	435	548, 578	1.03	0.78	−1.41	2.19
Compare:						
Re[T*p*CF_3PC](O)	438	552, 585	–	1.10	−1.16	2.26
Re[T*p*OCH_3PC](O)	441	556, 592	–	0.93	−1.29	2.22

macrocycle.[5,16,21,31−35] (In contrast, for noninnocent metallotriarylcorroles, the Soret maxima exhibit marked redshifts with increasing electron-donating character of the *para* substituent on the *meso*-phenyl groups.[25−30,36−42]) Moderately high oxidation potentials (0.8−1.0 V vs SCE) and low reduction potentials (−1.1 to −1.4 V), translating to an electrochemical HOMO−LUMO gap of ∼2.2 V, are also indicative of an innocent macrocycle and of purely ligand-centered oxidation and reduction processes.[30,43] Interestingly, both the oxidation and reduction potentials of the present imido complexes are some 100−150 mV downshifted relative to those of their oxo congeners,[16] an apparent reflection of the greater π-donating ability of the axial imido ligand.

Photophysical Studies. The photophysical properties of three of the Re-imido corroles, i.e., Re[T*p*CF_3PC](NPh), Re[TPC](NPh), and Re[T*p*OCH_3PC](NPh), were investigated in anoxic toluene at room temperature and in a 2:3 v/v toluene/tetrahydrofuran frozen glass at 77 K. In contrast to rather emissive ReO corroles,[14] the new Re-NPh complexes were found to be nonemissive at room temperature (Figure S19). However, experiments at 77 K revealed moderately strong phosphorescence (with quantum yields of 2.8−3.4%) of all the complexes (Figures 6, S20, and S21; Table 1). The emission of the Re-NPh corroles is located in the NIR part of the spectrum (λ_{max} = 749−761 nm), as for previously reported rhenium(V)-oxo corroles. The excitation spectra (Figures 6, S20, and S21) match very well with the absorption spectra of the dyes (Figure 4). At 77 K, the intensity decay profile is biexponential, with two components of around 45 and 100 μs (Table 3). Interestingly, the relative contributions of the components (∼33 and 67%, respectively) are very similar for all the dyes.

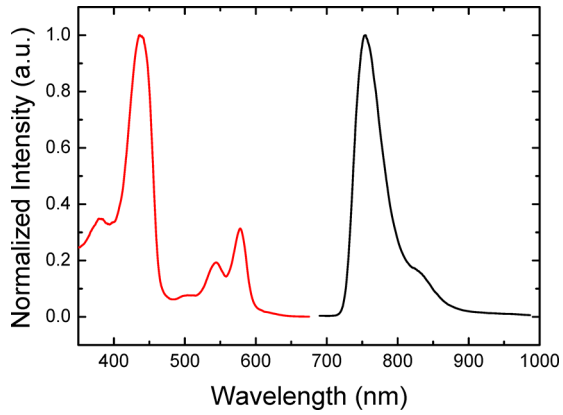

Figure 6. Excitation (red line, λ_{em}= 765 nm) and emission spectrum (black line, λ_{exc}= 440 nm) of Re(TPC)(NPh) in toluene/THF 4:6 v/v frozen glass at 77 K.

In addition to the photophysical studies, singlet oxygen sensitization was investigated for one of the new complexes, Re[TPC](NPh), using a literature method.[11,44] The method utilizes 9,10-dimethylanthracene as a singlet oxygen acceptor and methylene blue as a standard (whose quantum yield for singlet oxygen formation is 0.48). Formation of singlet oxygen by Re[TPC](NPh) was not detected (Figure S22). By comparison, we previously showed that even moderately phosphorescent $Os^{VI}N$ corroles are potent singlet oxygen sensitizers (quantum yields of singlet oxygen formation 0.76−

https://dx.doi.org/10.1021/acs.inorgchem.0c00477
Inorg. Chem. 2020, 59, 6382−6389

Table 3. Photophysical Properties of Re-imido Corroles at 77 K in a 4:6 v/v Toluene/THF Frozen Glass

complex	$\lambda_{max,ex}$ (nm)	$\lambda_{max,em}$ (nm)	Φ, %	τ (μs, % contribution)
Re[TPC](NPh)	437, 544, 578	754	2.8	41 (31%); 91 (69%)
Re[T*p*CF$_3$PC](NPh)	438, 544, 577	749	3.4	47 (34%); 108 (66%)
Re[T*p*OCH$_3$PC](NPh)	440, 546, 583	761	3.1	45 (34%); 89 (66%)

0.95).[11] Absence of singlet oxygen sensitization for Re[TPC](NPh) indicates very efficient deactivation of the triplet state in solution at room temperature, consistent with the absence of phosphorescence under the same conditions. Such efficient radiationless deactivation of the triplet state may result from rapid rotation of the axial phenyl substituent. As was mentioned above, phosphorescence does appear in a frozen glass at 77 K, where such rotation becomes impossible. Moreover, we also observed weak room-temperature phosphorescence after immobilization of the complex within a rigid matrix (polystyrene, Figure S23). Notably, polystyrene is rather similar to toluene in terms of polarity and its compatibility with the rhenium complex, and also to the frozen glass in terms of its presumed ability to inhibit rotation of the axial phenyl substituent. Interestingly, the intensity decay profile in polystyrene is monoexponential, with τ_0 = 75 μs (anoxic conditions).

CONCLUSION

In summary, we have developed a simple and general synthesis of Re-imido corroles, a welcome addition, in our opinion, in an area that is still bedeviled by capricious and low-yielding synthetic protocols. In addition to corrole peripheral substituents, the axial phenylimido group may provide an additional handle for structural diversification. Two single-crystal X-ray structures, electronic absorption spectra, and electrochemical studies are all strongly indicative of an innocent Re^{V}(NPh)-corrole^{3-} formulation for the new complexes. Interestingly, unlike several other classes of 5d metallocorroles, including ReO, OsN, Au, and Pt(IV) corroles, the Re-imido corroles proved nonemissive in anoxic toluene at room temperature. In a frozen glass at 77 K, however, they proved moderately phosphorescent, with quantum yields of 2.8−3.4%. The complexes also do not sensitize singlet oxygen formation in solution at room temperature, suggesting rapid radiationless deactivation of the triplet state, presumably as a result of rapid rotation of the axial phenyl group. By analogy with other metal-oxo and metal-imido corroles, we are optimiztic that the present complexes will help develop new axial ligation chemistry, an aspect of 5d metallocorroles that is still rather underdeveloped.

EXPERIMENTAL SECTION

Materials. Free-base *meso*-triarylcorroles were synthesized according to a literature procedure.[45] Dirhenium decacarbonyl, $Re_2(CO)_{10}$, aniline, 1,2,4-trichlorobenzene, potassium carbonote granulated, K_2CO_3 were purchased from Sigma-Aldrich and used as received. A sealable 20 mL microwave vial was used for the synthesis. Silica gel 60 (0.04−0.063 mm particle size, 230−400 mesh, Merck) was used for flash chromatography and silica gel 60 preparative thin-layer chromatography (PTLC) plates (20 cm × 20 cm, 0.5 mm thick; Merck) were used for final purification of all complexes.

Standard Analytical Methods. UV−visible−NIR spectra were recorded on an HP 8453 spectrophotometer. ^{1}H NMR spectra were recorded on 400 MHz Bruker Avance III HD spectrometer equipped with a 5 mm BB/^{1}H SmartProbe at 253 K in $CDCl_3$ or CD_2Cl_2 and referenced to residual $CHCl_3$ at 7.26 ppm and CH_2Cl_2 at 5.31 ppm. Mass spectra were recorded on a Thermo Scientific LTQ Orbitrap XL spectrometer with an ION-MAX electrospray ion source in positive mode.

Cyclic voltammetry was carried out at 298 K with an EG&G Model 263A potentiostat having a three-electrode system−a glassy carbon working electrode, a platinum wire counterelectrode, and a saturated calomel reference electrode (SCE). Anhydrous CH_2Cl_2 (Aldrich) was used as solvent and tetrakis(*n*-butyl)ammonium perchlorate, recrystallized twice from absolute ethanol, and dried in a desiccator for at least 2 weeks, was used as the supporting electrolyte. The reference electrode was separated from the bulk solution using a fritted-glass bridge filled with the solvent/supporting-electrolyte mixture. The electrolyte solution was purged with argon for at least 2 min, and all measurements were carried out under an argon blanket. All potentials were referenced to the SCE. Elemental analyses were obtained from Atlantic Microlab, Inc.

General Procedure for the Synthesis of Re[T*p*XPC](NPh). To a 20 mL microwave vial containing 1,2,4-trichlorobenzene (10 mL) and a magnetic stirring bar was added a free-base corrole, H_3[T*p*XPC] or H_3TPFPC (0.125 mmol), $Re_2(CO)_{10}$ (0.25 mmol), aniline (0.3 mL), and potassium carbonate (100 mg). The contents were sealed and deoxygenated with a flow of argon (via needles) for 10 min. The argon line was removed, and the vial was heated in an oil bath at 190 °C for 16 h with constant stirring. Completion of the reaction was indicated by the disappearance of the Soret absorption of the free-base corrole and appearance of a new Soret maximum at ∼436 nm. Upon cooling, the reaction mixture was loaded directly on to silica gel column with *n*-hexane as the mobile phase. The 1,2,4-trichlorobenzene was first removed by eluting with pure hexane. Different solvent mixtures were then used to elute the various reddish Re-imido/ReO corrole mixtures, namely, 3:1 v/v *n*-hexane/dichloromethane for X = CF_3, H, CH_3, F, and for TPFPC; 2:1 v/v *n*-hexane/dichloromethane for X = OCH_3. All fractions with λ_{max} ∼ 436 nm were collected and dried. The resulting products, which still consisted of mixtures of Re-imido and ReO corroles, were then subjected to preparative thin-layer chromatography on silica plates with 3:1 *n*-hexane/dichloromethane (for X = CF_3, H, CH_3, F, and TPFPC) or 2:1 *n*-hexane/dichloromethane (for X = OCH_3). The first light-red band corresponded to the desired Re-imido corroles and a second dark-red band to the ReO corroles.

X-ray quality crystals of the two Re-imido corroles (X = F and CF_3) were obtained by slow diffusion of methanol vapor into concentrated benzene solutions of the complexes. The yields and analytical details for the different Re-imido corroles are as follows.

Re[TPFPC](NPh). Yield: 46.76 mg (34.8%). UV−vis (CH_2Cl_2): λ_{max} [nm, $\varepsilon \times 10^{-4}$ (M^{-1} cm^{-1})]: 266 (3.05), 431 (7.10), 544 (0.96), 577 (1.00). ^{1}H NMR (400 MHz, −20 °C): δ 9.56 (d, 2H, $^3J_{HH}$ = 4.40 Hz, *β*-H); 9.15 (d, 2H, $^3J_{HH}$ = 4.28 Hz, *β*-H); 9.10 (d, 2H, $^3J_{HH}$ = 4.64 Hz, *β*-H); 8.99 (d, 2H, $^3J_{HH}$ = 4.76 Hz, *β*-*H*); 6.32 (t, 1H, $^3J_{HH}$ = 7.32 Hz, *p*-NPh); 6.11 (t, 2H, $^3J_{HH}$ = 7.76 Hz, *m*-NPh); 4.35 (d, 2H, $^3J_{HH}$ = 7.92 Hz, *o*-NPh); ^{19}F NMR: −136.60 (d, 2F, $^3J_{FF}$ = 26.52, 5,15-*o*1-Ph); −136.76 (d, 1F, $^3J_{FF}$ = 26.12 Hz Hz, 10-*o*1-Ph); −137.50 (d, 2F, $^3J_{FF}$ = 12.12 Hz, 5,15-*o*2-Ph); −137.57 (d, 1F, $^3J_{FF}$ = 9.16 Hz, 10-*o*2-Ph); −151.91 (m, 3F, 5,10,15-*p*-Ph); −161.05 (m, 6F, 5,10,15-*m*-Ph). MS (ESI): M^+ = 1071.0513 (exp.), 1071.0498 (calcd for $C_{43}H_{13}F_{15}N_5Re$); elemental analysis calcd for $C_{43}H_{13}F_{15}N_5Re$: C 48.23, H 1.22, N 6.54; found: C 48.47, H 1.65, N 5.99.

Re[T*p*CF$_3$PC](NPh). Yield: 43.33 mg (34.36%). UV−vis (CH_2Cl_2): λ_{max} [nm, $\varepsilon \times 10^{-4}$ (M^{-1} cm^{-1})]: 269 (391), 434 (7.98), 547 (1.18), 577 (1.40). ^{1}H NMR (400 MHz, −20 °C): δ 9.53 (d, 2H, $^3J_{HH}$ = 4.28 Hz, *β*-H); 9.17 (d, 4H, $^3J_{HH}$ = 4.20 Hz, *β*-H); 8.96 (d, 2H, $^3J_{HH}$ = 4.80 Hz, *β*-H); 8.75 (d, 2H, $^3J_{HH}$ = 7.88 Hz, 5,15-*o*1-Ph); 8.62 (d, 1H, $^3J_{HH}$ = 8 Hz, 10-*o*1-Ph); 8.15 (overlapping doublets, 5H, 10-*o*2-Ph, 5,15-*o*2-Ph, and 5,15-*m*1-Ph); 8.03 (overlapping doublets, 4H, 5,15-*m*2-Ph, 10-*m*1, and *m*2-Ph); 6.43 (t, 1H, $^3J_{HH}$ =

https://dx.doi.org/10.1021/acs.inorgchem.0c00477
Inorg. Chem. 2020, 59, 6382−6389

7.28 Hz, *p*-NPh); 6.20 (t, 2H, $^3J_{HH}$ = 7.72 Hz, *m*-NPh); 4.42 (d, 2H, $^3J_{HH}$ = 7.92 Hz, *o*-NPh). MS (ESI): M^+ = 1005.1548 (exp.), 1005.1529 (calcd for $C_{46}H_{25}N_5F_9Re$); elemental analysis calcd for $C_{46}H_{25}N_5Re$: C 54.98, H 2.51, N 6.97; found: C 54.68, H 2.32, N 7.12.

Re[T*p*FPC](NPh). Yield: 37.49 mg (35.08%). UV−vis (CH_2Cl_2): λ_{max} [nm, $\varepsilon \times 10^{-4}$ (M^{-1} cm^{-1})]: 272 (3.83), 434 (7.54), 548 (1.19), 575 (1.45). ^{1}H NMR (400 MHz, −20 °C): δ 9.48 (d, 2H, $^3J_{HH}$ = 4.32 Hz, β-H); 9.16 (d, 4H, $^3J_{HH}$ = 5.02 Hz, β-H); 8.97 (d, 2H, $^3J_{HH}$ = 4.80 Hz, β-H); 8.57 (m, 2H, 5,15-*o*1-Ph); 8.44 (m, 1H, 10-*o*1-Ph); 7.96 (m, 2H, 5,15-*o*2-Ph); 7.84 (m, 1H, 10-*o*2-Ph); 7.58 (m, 3H, 5,10,15-*m*1-Ph); 7.45 (m, 3H, 5,10,15-*m*2-Ph); 6.41 (t, 1H, $^3J_{HH}$ = 7.24 Hz, *p*-NPh); 6.18 (t, 2H, $^3J_{HH}$ = 7.36 Hz, *m*-NPh); 4.41 (d, 2H, $^3J_{HH}$ = 7.80 Hz, *o*-NPh). MS (ESI): M^+ = 855.1631 (exp.), 855.1622 (calcd for $C_{43}H_{25}F_3N_5Re$); elemental analysis calcd for $C_{43}H_{25}F_3N_5Re$: C 60.41, H 2.95, N 8.19; found: C 60.16, H 3.42, N 7.78.

Re[TPC](NPh). Yield: 31.26 mg (31.22%). UV−vis (CH_2Cl_2): λ_{max} [nm, $\varepsilon \times 10^{-4}$ (M^{-1} cm^{-1})]: 271 (5.45), 434 (8.46), 548 (1.84), 576 (2.16). ^{1}H NMR (400 MHz, −20 °C): δ 9.47 (d, 2H, $^3J_{HH}$ = 4.36 Hz, β-H); 9.23 (d, 2H, $^3J_{HH}$ = 4.84 Hz, β-H); 9.19 (d, 2H, $^3J_{HH}$ = 4.32 Hz, β-H); 9.02 (d, 2H, $^3J_{HH}$ = 4.84 Hz, β-H); 8.60 (d, 2H, $^3J_{HH}$ = 7.52 Hz, 5,15-*o*1-Ph); 8.47 (d, 1H, $^3J_{HH}$= 6.96 Hz, 10-*o*1-Ph); 8.04 (d, 2H, $^3J_{HH}$ = 6.32 Hz, 5,15-*o*2-Ph); 7.94−7.68 (m, 10H, 10-*o*2-Ph; 5,15-*m*1 and *m*2-Ph; 10-*m*1 and *m*2-Ph; 5,10,15-*p*-Ph); 6.30 (t, 1H, $^3J_{HH}$= 6.68 Hz *p*-NPh); 6.10 (t, 2H, $^3J_{HH}$= 6.96 Hz, *m*-NPh); 4.35 (d, 2H, $^3J_{HH}$ = 8.32 Hz, *o*-NPh). MS (ESI): M^+ = 801.1911 (exp.), 801.1904 (calcd for $C_{43}H_{28}N_5Re$); elemental analysis calcd for $C_{43}H_{28}N_5Re{\cdot}H_2O$: C 63.06, H 3.69, N 8.55; found: C 62.70, H 3.82, N 8.27.

Re[T*p*CH$_3$PC](NPh). Yield: 29.75 mg (28.23%). UV−vis (CH_2Cl_2): λ_{max} [nm, $\varepsilon \times 10^{-4}$ (M^{-1} cm^{-1})]: 263 (5.22), 434 (7.85), 549 (1.77), 578 (2.09). ^{1}H NMR (400 MHz, −20 °C): δ 9.47 (d, 2H, $^3J_{HH}$ = 4.24 Hz, β-H); 9.20 (d, 2H, $^3J_{HH}$ = 3.84 Hz, β-H); 9.17 (d, 2H, $^3J_{HH}$ = 4.20 Hz, β-H); 8.99 (d, 2H, $^3J_{HH}$ = 4.80 Hz, β-H); 8.46 (d, 2H, $^3J_{HH}$ = 7.48 Hz, 5,15-*o*1-Ph); 8.32 (d, 1H, $^3J_{HH}$= 7.00 Hz, 10-*o*1-Ph); 7.91 (d, 2H, $^3J_{HH}$ = 7.48 Hz, 5,15-*o*2-Ph); 7.77 (d, 1H, $^3J_{HH}$ = 8.00 Hz, 10-*o*2-Ph); 7.69 (d, 2H, $^3J_{HH}$ = 7.12 Hz, 5,15-*m*1-Ph); 7.62 (d, 1H, $^3J_{HH}$ = 7.96 Hz, 10-*m*1-Ph); 7.55 (d, 2H, $^3J_{HH}$ = 7.40 Hz, 5,15-*m*2-Ph); 7.49 (d, 1H, $^3J_{HH}$ = 7.40 Hz, 10-*m*2-Ph); 6.33 (t, 1H, $^3J_{HH}$ = 6.64 Hz, *p*-NPh); 6.12 (t, 2H, $^3J_{HH}$ = 5.84 Hz, *m*-NPh); 4.34 (d, 2H, $^3J_{HH}$ = 7.60 Hz, *o*-NPh); 2.66 (s, 6H, 5,15-*p*-CH_3); 2.65 (s, 3H, 10-*p*-CH_3). MS (ESI): M^+ = 843.2387 (exp.), 843.2374 (calcd for $C_{46}H_{34}N_5Re$); elemental analysis calcd for $C_{46}H_{34}N_5Re$: C 65.54, H 4.07, N 8.31; found: C 65.19, H 4.27, N 8.01.

Re[T*p*OCH$_3$PC](NPh). Yield: 30.86 mg (27.71%). UV−vis (CH_2Cl_2): λ_{max} [nm, $\varepsilon \times 10^{-4}$ (M^{-1} cm^{-1})]: 164 (5.72), 435 (8.17), 548 (1.73), 578 (2.10). ^{1}H NMR (400 MHz, −20 °C): δ 9.46 (d, 2H, $^3J_{HH}$ = 4.64 Hz, β-H); 9.22 (d, 2H, $^3J_{HH}$ = 5.00 Hz, β-H); 9.17 (d, 2H, $^3J_{HH}$ = 4.16 Hz, β-H); 9.01 (d, 2H, $^3J_{HH}$ = 4.88 Hz, β-H); 8.49 (d, 2H, $^3J_{HH}$ = 8.32 Hz, 5,15-*o*1-Ph); 8.35 (d, 1H, $^3J_{HH}$ = 9.04 Hz, 10-*o*1-Ph); 7.95 (d, 2H, $^3J_{HH}$ = 8.44 Hz, 5,15-*o*2-Ph); 7.81 (d, 1H, $^3J_{HH}$ = 8.56 Hz, 10-*o*2-Ph); 7.39 (d, 2H, $^3J_{HH}$ = 0.08 Hz, 5,15-*m*1-Ph); 7.33 (d, 1H, $^3J_{HH}$ = 9.52 Hz, 10-*m*1-Ph); 7.26 (d, 2H, $^3J_{HH}$ = 9.52 Hz, 5,15-*m*2-Ph); 7.20 (d, 1H, $^3J_{HH}$ = 9.20 Hz, 10-*m*2-Ph); 6.34 (t, 1H, $^3J_{HH}$ = 6.52 Hz, *p*-NPh); 6.13 (t, 2H, $^3J_{HH}$ = 7.84 Hz, *m*-NPh); 4.34 (d, 2H, $^3J_{HH}$ = 8.80 Hz, *o*-NPh); 4.02 (s, 6H, 5,15-*p*-OCH_3); 4.00 (s, 3H, 10-*p*-OCH_3). MS (ESI): M^+ = 891.2236 (exp.), 891.2222 (calcd for $C_{46}H_{34}O_3N_5Re$); elemental analysis calcd for $C_{46}H_{34}N_5O_3Re{\cdot}H_2O$: C 60.78, H 3.99, N 7.70; found: C 60.77, H 4.18, N 7.55.

X-ray Crystallographic Analyses. X-ray data for Re[TPFPC](NPh) and Re[T*p*CF$_3$PC](NPh) were collected on beamline 12.2.1 at the Advanced Light Source, Lawrence Berkeley National Laboratory. Each crystal was mounted on a MiTeGen kapton loop and placed in a nitrogen cold stream provided by an Oxford Cryostream 800 Plus low-temperature apparatus on the goniometer head of a Bruker D8 diffractometer equipped with a PHOTONII CPAD detector operating in shutterless mode. All diffraction data were collected with synchrotron radiation monochromated using silicon(111) to a wavelength of 0.7288(1) Å. An approximate full-sphere of data was collected for each crystal using a combination of phi and omega scans. The crystals of Re[T*p*CF$_3$PC](NPh) were found to be twinned, and the components were separated using the CELL_NOW program.[46] Absorption corrections were applied with SADABS[47] for Re[T*p*FPC](NPh) and with TWINABS[48] for Re[T*p*CF$_3$PC](NPh). The structures were solved by dual space (SHELXT)[49] and refined by full-matrix least-squares on F^2 (SHELXL-2018).[50] All non-hydrogen atoms were refined anisotropically. Hydrogen atoms were geometrically calculated and refined as riding atoms.

For Re[T*p*CF$_3$PC](NPh), CELL_NOW was used to determined the two orientation matices. The relationship between the components was found to be 180° about the reciprocal axis 1 0 0. The data were integrated using the two matrices in SAINT and TWINABS was used to produce a merged HKLF4 file for structure solution and initial refinement and an HKLF5 file for final structure refinement. TWINABS indicated the twin ratio to be 83:17. Displacement parameter restraints were used to model the CF_3 group containing C40, F7−F9, and F7′−F9′.

Photophysical Studies. The photophysical properties of the Re-imido corroles were measured on a Fluorolog 3 fluorescence spectrometer (Horiba, Japan) equipped with an NIR-sensitive R2658 photomultiplier (Hamamatsu, Japan). The spectra were corrected for the sensitivity of the photomultiplier and smoothing was (adjusting averaging function) applied to eliminate noise due to low signals. For measurements in toluene, the dye solutions in a sealable quartz cell (Hellma Analytics, Mülheim, Germany) were deoxygenated by bubbling argon (5.0, Linde gas, Austria) for 15 min. Measurements at 77K were conducted in a 2:3 v/v toluene/tetrahydrofuran frozen glass using low-temperature accessories from Horiba. Luminescence quantum yields under these conditions were evaluated relative to *N*,*N*′-bis(2,6-diisopropylphenyl)-1,6,7,12-tetraphenoxyperylene-3,4,9,10-tetracarboxylic acid diimide ("fluorescent red", Kremer Pigmente, Germany), assuming Φ = 100% in toluene/tetrahydrofuran glass at 77 K (Φ = 96% in chloroform at room temperature).[51] The excitation wavelength of 543 nm was used for all the complexes and the reference dye. Luminescence decay times were measured on the Fluorolog 3 spectrometer equipped with a DeltaHub module (Horiba Scientific) controlling a SpectraLED-460 lamp and with DAS-6 software for data analysis.

Singlet oxygen generation by Re[TPC](NPh) was studied using a previously described protocol.[11] The assay makes use of 9,10-dimethylanthracene, which as a singlet oxygen acceptor decomposes at a rate proportional to the singlet oxygen quantum yield of the sensitizer.

■ ASSOCIATED CONTENT

Supporting Information

The Supporting Information is available free of charge at https://pubs.acs.org/doi/10.1021/acs.inorgchem.0c00477.

Electrospray ionization mass spectra (PDF)

Accession Codes

CCDC 1967816−1967817 contain the supplementary crystallographic data for this paper. These data can be obtained free of charge via www.ccdc.cam.ac.uk/data_request/cif, or by emailing data_request@ccdc.cam.ac.uk, or by contacting The Cambridge Crystallographic Data Centre, 12 Union Road, Cambridge CB2 1EZ, UK; fax: +44 1223 336033.

■ AUTHOR INFORMATION

Corresponding Author

Abhik Ghosh − *Department of Chemistry, UiT—The Arctic University of Norway, N-9037 Tromsø, Norway;* orcid.org/0000-0003-1161-6364; Email: abhik.ghosh@uit.no

https://dx.doi.org/10.1021/acs.inorgchem.0c00477
Inorg. Chem. 2020, 59, 6382−6389

Authors

Abraham B. Alemayehu − *Department of Chemistry, UiT—The Arctic University of Norway, N-9037 Tromsø, Norway;* orcid.org/0000-0003-0166-8937

Simon J. Teat − *Advanced Light Source, Lawrence Berkeley National Laboratory, Berkeley, California 94720-8229, United States*

Sergey M. Borisov − *Institute of Analytical Chemistry and Food Chemistry, Graz University of Technology, 8010 Graz, Austria;* orcid.org/0000-0001-9318-8273

Complete contact information is available at: https://pubs.acs.org/10.1021/acs.inorgchem.0c00477

Notes

The authors declare no competing financial interest.

■ ACKNOWLEDGMENTS

This work was supported by NANO2021 (262229) of the Research Council of Norway (A.G.) and used resources of the Advanced Light Source, which is a DOE Office of Science User Facility under contract no. DE-AC02-05CH11231.

■ REFERENCES

(1) Ghosh, A. Electronic Structure of Corrole Derivatives: Insights from Molecular Structures, Spectroscopy, Electrochemistry, and Quantum Chemical Calculations. *Chem. Rev.* **2017**, *117*, 3798−3881.

(2) Nardis, S.; Mandoj, F.; Stefanelli, M.; Paolesse, R. Metal complexes of corrole. *Coord. Chem. Rev.* **2019**, *388*, 360−405.

(3) Alemayehu, A. B.; Ghosh, A. Gold Corroles. *J. Porphyrins Phthalocyanines* **2011**, *15*, 106−110.

(4) Rabinovich, E.; Goldberg, I.; Gross, Z. Gold(I) and Gold(III) Corroles. *Chem. - Eur. J.* **2011**, *17*, 12294−12301.

(5) Thomas, K. E.; Alemayehu, A. B.; Conradie, J.; Beavers, C.; Ghosh, A. Synthesis and Molecular Structure of Gold Triarylcorroles. *Inorg. Chem.* **2011**, *50*, 12844−12851.

(6) Thomas, K. E.; Vazquez-Lima, H.; Fang, Y.; Song, Y.; Gagnon, K. J.; Beavers, C. M.; Kadish, K. M.; Ghosh, A. Ligand Noninnocence in Coinage Metal Corroles: A Silver Knife-Edge. *Chem. - Eur. J.* **2015**, *21*, 16839−16847.

(7) Alemayehu, A. B.; Vazquez-Lima, H.; Beavers, C. M.; Gagnon, K. J.; Bendix, J.; Ghosh, A. Platinum Corroles. *Chem. Commun.* **2014**, *50*, 11093−11096.

(8) Alemayehu, A. B.; McCormick, L. J.; Gagnon, K. J.; Borisov, S. M.; Ghosh, A. Stable Platinum(IV) Corroles: Synthesis, Molecular Structure, and Room-Temperature Near-IR Phosphorescence. *ACS Omega* **2018**, *3*, 9360−9368.

(9) Palmer, J. H.; Durrell, A. C.; Gross, Z.; Winkler, J. R.; Gray, H. B. Near-IR Phosphorescence of Iridium(III) Corroles at Ambient Temperature. *J. Am. Chem. Soc.* **2010**, *132*, 9230−9231.

(10) Sinha, W.; Ravotto, L.; Ceroni, P.; Kar, S. NIR-Emissive Iridium(III) Corrole Complexes as Efficient Singlet Oxygen Sensitizers. *Dalton Trans.* **2015**, *44*, 17767−73.

(11) Borisov, S. M.; Alemayehu, A.; Ghosh, A. Osmium-Nitrido Corroles as NIR Indicators for Oxygen Sensors and Triplet Sensitizers for Organic Upconversion and Singlet Oxygen Generation. *J. Mater. Chem. C* **2016**, *4*, 5822−5828.

(12) Lemon, C. M.; Powers, D. C.; Brothers, P. J.; Nocera, D. G. Gold Corroles as Near-IR Phosphors for Oxygen Sensing. *Inorg. Chem.* **2017**, *56*, 10991−10997.

(13) Alemayehu, A. B.; Day, N. U.; Mani, T.; Rudine, A. B.; Thomas, K. E.; Gederaas, O. A.; Vinogradov, S. A.; Wamser, C. C.; Ghosh, A. Gold Tris(carboxyphenyl)corroles as Multifunctional Materials: Room Temperature Near-IR Phosphorescence and Applications to Photodynamic Therapy and Dye-Sensitized Solar Cells. *ACS Appl. Mater. Interfaces* **2016**, *8*, 18935−18942.

(14) Borisov, S. M.; Einrem, R. F.; Alemayehu, A. B.; Ghosh, A. Ambient-temperature near-IR phosphorescence and potential applications of rhenium-oxo corroles. *Photochem. Photobiol. Sci.* **2019**, *18*, 1166−1170.

(15) Teo, R. D.; Hwang, J. Y.; Termini, J.; Gross, Z.; Gray, H. B. Fighting Cancer with Corroles. *Chem. Rev.* **2017**, *117*, 2711−2729.

(16) Einrem, R. F.; Gagnon, K. J.; Alemayehu, A. B.; Ghosh, A. Metal-Ligand Misfits: Facile Access to Rhenium-Oxo Corroles by Oxidative Metalation. *Chem. - Eur. J.* **2016**, *22*, 517−520.

(17) Schweyen, P.; Brandhorst, K.; Hoffmann, M.; Wolfram, B.; Zaretzke, M.-K.; Bröring, M. Viking Helmet Corroles: Activating Inert Oxidometal Corroles. *Chem. - Eur. J.* **2017**, *23*, 13897−13900.

(18) Ziegler, J. A.; Buckley, H. L.; Arnold, J. Synthesis and reactivity of tantalum corrole complexes. *Dalton Trans.* **2017**, *46*, 780−785.

(19) Buckley, H. L.; Arnold, J. Recent developments in out-of-plane metallocorrole chemistry across the periodic table. *Dalton Trans.* **2015**, *44*, 30−36.

(20) Reinholdt, A.; Alemayehu, A. B.; Gagnon, K. J.; Bendix, J.; Ghosh, A. Electrophilic Activation of Osmium-Nitrido Corroles. The OsN Triple Bond as a π-Acceptor Metalla-Ligand in a Heterobimetallic $Os^{VI}N\text{-}Pt^{II}$ Complex. *Inorg. Chem.* **2020**, DOI: 10.1021/acs.inorgchem.0c00654.

(21) Alemayehu, A. B.; Gagnon, K. J.; Terner, J.; Ghosh, A. Oxidative Metalation as a Route to Size-Mismatched Macrocyclic Complexes: Osmium Corroles. *Angew. Chem., Int. Ed.* **2014**, *53*, 14411−14414.

(22) Pyykkö, P.; Riedel, S.; Patzschke, M. Triple-Bond Covalent Radii. *Chem. - Eur. J.* **2005**, *11*, 3511−3520.

(23) Pyykkö, P.; Atsumi, M. Molecular Single-Bond Covalent Radii for Elements 1−118. *Chem. - Eur. J.* **2009**, *15*, 186−197.

(24) Pyykkö, P.; Atsumi, M. Molecular Double-Bond Covalent Radii for Elements Li−E112. *Chem. - Eur. J.* **2009**, *15*, 12770−12779.

(25) Steene, E.; Wondimagegn, T.; Ghosh, A. Electrochemical and Electronic Absorption Spectroscopic Studies of Substituent Effects in Iron(IV) and Manganese(IV) Corroles. Do the Compounds Feature High-Valent Metal Centers or Noninnocent Corrole Ligands? Implications for Peroxidase Compound I and II Intermediates. *J. Phys. Chem. B* **2001**, *105*, 11406−11413; *J. Phys. Chem. B* **2002**, *106*, 5312−5312.

(26) Vazquez-Lima, H.; Norheim, H. K.; Einrem, R. F.; Ghosh, A. Cryptic Noninnocence: FeNO Corroles in a New Light. *Dalton Trans.* **2015**, *44*, 10146−10151.

(27) Norheim, H.-K.; Capar, J.; Einrem, R. F.; Gagnon, K. J.; Beavers, C. M.; Vazquez-Lima, H.; Ghosh, A. Ligand Noninnocence in FeNO Corroles: Insights from β-Octabromocorrole Complexes. *Dalton Trans.* **2016**, *45*, 681−689.

(28) Ganguly, S.; McCormick, L. J.; Conradie, J.; Gagnon, K. J.; Sarangi, R.; Ghosh, A. Electronic Structure of Manganese Corroles Revisited: X-ray structures, Optical and X-ray Absorption Spectroscopies, and Electrochemistry as Probes of Ligand Noninnocence. *Inorg. Chem.* **2018**, *57*, 9656−9669.

(29) Ganguly, S.; Vazquez-Lima, H.; Ghosh, A. Wolves in Sheep's Clothing: μ-Oxo-Diiron Corroles Revisited. *Chem. - Eur. J.* **2016**, *22*, 10336−10340.

(30) Ganguly, S.; Ghosh, A. Seven Clues to Ligand Noninnocence: The Metallocorrole Paradigm. *Acc. Chem. Res.* **2019**, *52* (7), 2003−2014.

(31) Johansen, I.; Norheim, H.-K.; Larsen, S.; Alemayehu, A. B.; Conradie, J.; Ghosh, A. Substituent effects on metallocorrole spectra: insights from chromium-oxo and molybdenum-oxo triarylcorroles. *J. Porphyrins Phthalocyanines* **2011**, *15*, 1335−1344.

(32) Einrem, R. F.; Braband, H.; Fox, T.; Vazquez-Lima, H.; Alberto, R.; Ghosh, A. Synthesis and Molecular Structure of ^{99}Tc Corroles. *Chem. - Eur. J.* **2016**, *22*, 18747−18751.

(33) Alemayehu, A. B.; Vazquez-Lima, H.; Gagnon, K. J.; Ghosh, A. Stepwise Deoxygenation of Nitrite as a Route to Two Families of Ruthenium Corroles: Group 8 Periodic Trends and Relativistic Effects. *Inorg. Chem.* **2017**, *56*, 5285−5294.

(34) Alemayehu, A.; Vazquez-Lima, H.; McCormick, L. J.; Ghosh, A. Relativistic effects in metallocorroles: comparison of molybdenum and tungsten biscorroles. *Chem. Commun.* **2017**, *53*, 5830−5833.
(35) Alemayehu, A.; Vazquez-Lima, H.; Gagnon, K. J.; Ghosh, A. Tungsten Biscorroles: New Chiral Sandwich Compounds. *Chem. - Eur. J.* **2016**, *22*, 6914−6920.
(36) Wasbotten, I. H.; Wondimagegn, T.; Ghosh, A. Electronic Absorption, Resonance Raman, and Electrochemical Studies of Planar and Saddled Copper(III) *Meso*-Triarylcorroles. Highly Substituent-Sensitive Soret Bands as a Distinctive Feature of High-Valent Transition Metal Corroles. *J. Am. Chem. Soc.* **2002**, *124*, 8104−8116.
(37) Alemayehu, A. B.; Gonzalez, E.; Hansen, L. K.; Ghosh, A. Copper Corroles Are Inherently Saddled. *Inorg. Chem.* **2009**, *48*, 7794−7799.
(38) Alemayehu, A. B.; Hansen, L. K.; Ghosh, A. Nonplanar, Noninnocent, and Chiral: A Strongly Saddled Metallocorrole. *Inorg. Chem.* **2010**, *49*, 7608−7610.
(39) Thomas, K. E.; Wasbotten, I. H.; Ghosh, A. Copper *β*-Octakis(Trifluoromethyl)Corroles: New Paradigms for Ligand Substituent Effects in Transition Metal Complexes. *Inorg. Chem.* **2008**, *47*, 10469−10478.
(40) Alemayehu, A. B.; Conradie, J.; Ghosh, A. A First TDDFT Study of Metallocorrole Electronic Spectra: Copper *meso*-Triarylcorroles Exhibit *Hyper* Spectra. *Eur. J. Inorg. Chem.* **2011**, *2011*, 1857−1864.
(41) Berg, S.; Thomas, K. E.; Beavers, C. M.; Ghosh, A. Undecaphenylcorroles. *Inorg. Chem.* **2012**, *51*, 9911−9916.
(42) Thomas, K. E.; Vazquez-Lima, H.; Fang, Y.; Song, Y.; Gagnon, K. J.; Beavers, C. M.; Kadish, K. M.; Ghosh, A. Ligand Noninnocence in Coinage Metal Corroles: A Silver Knife-Edge. *Chem. - Eur. J.* **2015**, *21*, 16839−16847.
(43) Fang, Y.; Ou, Z.; Kadish, K. M. Electrochemistry of Corroles in Nonaqueous Media. *Chem. Rev.* **2017**, *117*, 3377−3419.
(44) Gross, E.; Ehrenberg, B.; Johnson, F. M. Singlet oxygen generation by porphyrins and the kinetics of 9,10-dimethylanthracene photosensitization in liposomes. *Photochem. Photobiol.* **1993**, *57*, 808−813.
(45) Koszarna, B.; Gryko, D. T. Efficient Synthesis of *meso*-Substituted Corroles in a H_2O-MeOH Mixture. *J. Org. Chem.* **2006**, *71*, 3707−3717.
(46) *CELL_NOW: Index Twins and Other Problem Crystals*, version 2008/4; Bruker: 2016.
(47) Krause, L.; Herbst-Irmer, R.; Sheldrick, G. M.; Stalke, D. Comparison of silver and molybdenum microfocus X-ray sources for single-crystal structure determination. *J. Appl. Crystallogr.* **2015**, *48*, 3−10.
(48) *TWINABS: Bruker AXS Scaling for Twinned Crystals*, version 2012/1; Bruker: 2016.
(49) Sheldrick, G. M. SHELXT - Integrated Space-Group and Crystal-Structure Determination. *Acta Crystallogr., Sect. A: Found. Adv.* **2015**, *A71*, 3−8.
(50) Sheldrick, G. M. Crystal Structure Refinement with SHELXL. *Acta Crystallogr., Sect. C: Struct. Chem.* **2015**, *C71*, 3−8.
(51) Seybold, G.; Wagenblast, G. New perylene and violanthrone dyestuffs for fluorescent collectors. *Dyes Pigm.* **1989**, *11*, 303−317.

https://dx.doi.org/10.1021/acs.inorgchem.0c00477
Inorg. Chem. 2020, 59, 6382−6389